Zeitschrift: Helvetica Physica Acta
Band: 61 (1988)
Heft: 4

Artikel: H_c2-anisotropy effects in superconducting niobium polycrystals
Autor: Weber, H.W. / Schachinger, E.
DOI: https://doi.org/10.5169/seals-115952

Nutzungsbedingungen

Die ETH-Bibliothek ist die Anbieterin der digitalisierten Zeitschriften auf E-Periodica. Sie besitzt keine Urheberrechte an den Zeitschriften und ist nicht verantwortlich für deren Inhalte. Die Rechte liegen in der Regel bei den Herausgebern beziehungsweise den externen Rechteinhabern. Das Veröffentlichen von Bildern in Print- und Online-Publikationen sowie auf Social Media-Kanälen oder Webseiten ist nur mit vorheriger Genehmigung der Rechteinhaber erlaubt. Mehr erfahren

Conditions d'utilisation

L'ETH Library est le fournisseur des revues numérisées. Elle ne détient aucun droit d'auteur sur les revues et n'est pas responsable de leur contenu. En règle générale, les droits sont détenus par les éditeurs ou les détenteurs de droits externes. La reproduction d'images dans des publications imprimées ou en ligne ainsi que sur des canaux de médias sociaux ou des sites web n'est autorisée qu'avec l'accord préalable des détenteurs des droits. En savoir plus

Terms of use

The ETH Library is the provider of the digitised journals. It does not own any copyrights to the journals and is not responsible for their content. The rights usually lie with the publishers or the external rights holders. Publishing images in print and online publications, as well as on social media channels or websites, is only permitted with the prior consent of the rights holders. Find out more

Download PDF: 10.01.2026

ETH-Bibliothek Zürich, E-Periodica, https://www.e-periodica.ch

Helvetica Physica Acta, Vol. **61** (1988) 478–487

0018–0238/88/040478–10\$1.50 + 0.20/0

H_{c2}-anisotropy effects in superconducting niobium polycrystals

By H. W. Weber

Atominstitut der Österreichischen Universitäten, A-1020 Vienna, Austria

and E. Schachinger

Institut für Theoretische Physik, Technische Universität, A-8010 Graz, Austria

(28. XII. 1987)

In honor of Martin Peter's 60th birthday.

Abstract. An extensive experimental study on the impurity dependence of superconductive properties in niobium has been made. In the present paper we will concentrate on those results pertaining to the temperature and impurity dependence of the upper critical fields H_{c2} in a range of impurity parameters from 0.01 to 0.72. Brief reference will be made to the influence of anisotropies on the thermodynamics of these materials. The analysis of experimental results is made in terms of strong coupling theory including anisotropies via separable model potentials. In the case of H_{c2}, two mean square anisotropy parameters are obtained, namely $\langle a^2 \rangle = 0.033$ for the electron–phonon interaction anisotropy and $\langle b^2 \rangle = 0.118$ for the anisotropy of the Fermi velocity v_F. v_F itself is found to be $5.7 \cdot 10^5$ m/s. Using these parameters, the overall agreement between the experimental and theoretical critical field curves is better than 2% in the entire range of temperatures and impurity concentrations. Furthermore, these parameters agree very well with previous work on the Fermi surface anisotropy in niobium.

1. Introduction

For many years experimental as well as theoretical investigations have been aimed at an unambiguous assessment of the existence and magnitude of anisotropies in the electron–phonon interaction caused by real metal effects in various superconductors [1]. Although it is obvious that these effects should be most clearly detectable in high-purity singlecrystalline materials, where specific properties can be mapped as a function of crystal directions, most of the experimental data turned out to be difficult to interpret in terms of the quantity of interest, namely the direction dependence of the electron–phonon interaction. These difficulties are either related to the experimental technique itself, as in the case of tunneling into single crystals [2], or to the lack of an appropriate means to deduce coupling anisotropies from the data. As an example of the latter case, measurements of H_{c2}-anisotropy in type-II superconductors should be mentioned in particular, because they refer to an easily accessible bulk property of the material and can be made with considerable accuracy [3–6].

In view of this unsatisfactory situation, a different approach, which, in fact, was used very early on, is attracting attention because of the availability of an appropriate theoretical treatment. In this case, the integral effect of anisotropies on various properties of the superconducting state in polycrystalline materials is studied and analyzed in terms of strong-coupling Eliashberg theory, including anisotropy effects in most cases via a separable pairing potential $V(k, k') = (1 + a_k)V_{BCS}(1 + a_{k'})$, where a_k is the temperature independent anisotropy parameter and V_{BCS} is the constant pairing potential of the BCS theory [7–11].

These principles have been applied recently [12] to an analysis of anisotropy effects on the thermodynamics of superconducting indium and provided an excellent consistent description of superconductivity in this material with considerable contributions of anisotropy (mean square anisotropy parameter $\langle a^2 \rangle = 0.035 \div 0.04$). However, because high accuracy data are needed, not only on the impurity dependence of the transition temperature T_c, but also on the temperature and impurity dependence of the thermodynamic critical field $H_c(T)$, this method is practically limited to type -I superconductors, where $H_c(T)$ is directly accessible to experiment.

With the development of an anisotropic strong coupling theory of upper critical fields H_{c2} [13–14], the precision of H_{c2} experiments can be combined with a mean-square anisotropy analysis in a broad range of materials, much along the lines discussed above for the thermodynamics of the superconducting state. In fact, both the anisotropy of the electron–phonon coupling as well as the anisotropy of the Fermi velocity are needed to analyze the experimental data. It is the purpose of the present paper to discuss for the first time the integral influence of both of these anisotropies on the upper critical field in a series of niobium polycrystals.

2. Experimental

2.1. *Materials*

As the starting materials, several polycrystalline rods and a [110]-oriented single crystal were purchased from Materials Research Corp., New York, U.S.A. The samples were cut into cylindrical form with a spark cutter and subjected to an initial degassing treatment in a UHV-system ($T = 2100$°C, base pressure: $\cong 10^{-11}$ mbar). As the next preparatory step, the materials were decarbonized in an oxygen atmosphere ($T = 1690$°C, $p_{02} = 10^{-8}$ mbar). Very high residual resistivity ratios of up to 2080 could be obtained in this way.

After these preparatory steps the samples were loaded with varying amounts of nitrogen in order to achieve the desired impurity variation within this system. This treatment was made at a fixed temperature of 2100°C for a fixed period of time (4 hours). The nitrogen partial pressure was varied between $6 \cdot 10^{-7}$ and $5 \cdot 10^{-4}$ mbar corresponding approximately to nitrogen concentrations in the

Table I
Material parameters for the system niobium–nitrogen. The values for $\langle b^2 \rangle$ and $\langle v_F \rangle$ are for the best possible fit. (C_{N2} is in at. % N_2, T_c in K, ρ_n in nΩm at 4.2 K, $\langle v_F \rangle$ in 10^6 ms^{-1} and $\alpha = 0.882\ \xi_0/l$.)

Sample	Nb8	Nb7	Nb4	Nb3	Nb5	Nb2
crystal	single	poly	poly	poly	poly	poly
C_{N2}	—	0.01	0.10	0.15	0.22	0.30
RRR	2080	385	57	38	26	20
$\rho_n \pm 2\%$	0.069	0.257	2.433	3.815	5.637	7.076
$T_c \pm 4$ mK	9.301	9.289	9.218	9.187	9.146	9.112
$\kappa(T_c)$	0.720	0.725	0.883	0.917	1.090	1.153
	±0.007	±0.010	±0.049	±0.015	±0.015	±0.045
α	0.011	0.020	0.278	0.421	0.616	0.719
ρ_0 (theor)	0.0927	0.381	2.44	3.587	5.429	7.325
$\langle b^2 \rangle$	0.111	0.112	0.118	0.125	0.125	0.125
$\langle v_F \rangle$	0.585	0.585	0.573	0.560	0.558	0.560
R (%)	14.9	14.5	12.3	11.2	10.1	9.1

range from 0.01 to 0.30 at $\% N_2$. As a final step the samples were exposed to a short heat treatment (400°C) in air, in order to reduce hysteresis effects associated with the surface barrier (cf. below).

A summary of relevant material parameters is presented in Table I.

2.2. *Measuring techniques*

Conventional four-point dc measurements were made at room temperature and at 4.2 K in order to determine the resistivities and residual resistivity ratios. The accuracy of this data is determined mainly by the extent to which the geometry of the sample can be assessed, and is estimated to be ±2%.

The major part of the experimental work refers to magnetization measurements using the differential technique with a low-temperature chopper [15]. Because of the excellent stability of this system, very low field-sweeping rates (0.1 mT/s) could be used in order to achieve true equilibrium conditions in the magnetization cycle. All the data were stored on a computer and analyzed numerically. The resolution for determining the upper critical field H_{c2} achieved from the differential curve, is normally better than ±0.5 mT. In all samples the magnetization was found to be sufficiently reversible, except for some irreversibilities near H_{c1} and occasional small peak effects near H_{c2} in samples doped with higher amounts of nitrogen. As an example, the integrated magnetization curves of samples Nb8 and Nb2 are shown in Fig. 1 for the initial magnetization and for decreasing fields.

In some cases the transition at H_{c2} was determined by an ac susceptibility technique [6] providing a field resolution of about ±50 μT.

3. Theory

It is well known from standard WHH theory [16] for the upper critical field and its strong coupling extension [17], that $H_{c2}(T)$ is solely determined by four

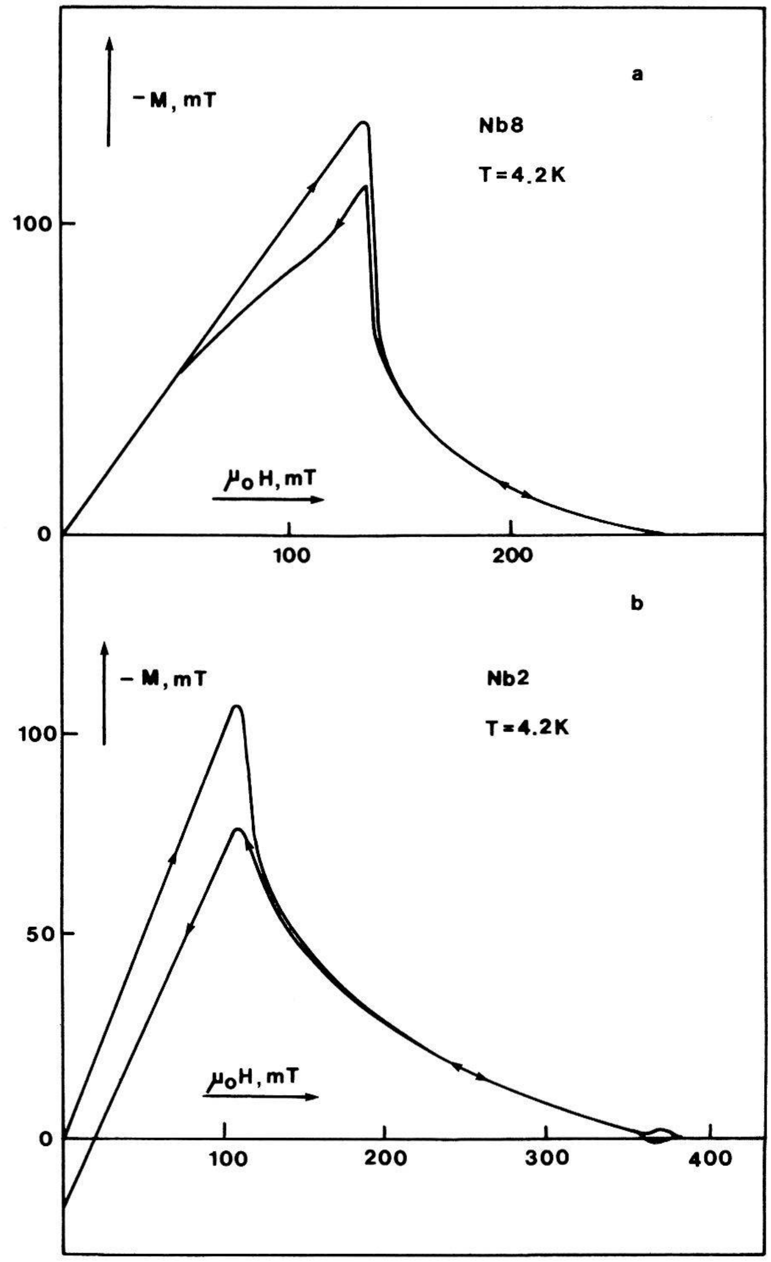

Figure 1
Integrated magnetization curves for samples Nb8 and Nb2, for the initial magnetization and for decreasing fields.

parameters: the electron–phonon interaction strength represented by the pairing potential V_{BCS}, or by the electron–phonon interaction spectral function $\alpha^2F(\omega)$, the transport relaxation time τ_{tr}, the Fermi velocity v_F and the Coulomb pseudopotential μ^*. The latter can be determined by *ab initio* calculations[18] or by simply fitting μ^* to the measured T_c of a particular sample for a given $\alpha^2F(\omega)$. The parameters v_F and τ_{tr} are usually 'free' parameters and are used to fit the initial slope of the $H_{c2}(T)$ curve (τ_{tr}) and the actual experimental values of H_{c2} (v_F).

If there is only s-wave scattering by non-magnetic impurities, it is possible to relate τ_{tr} to the residual resistivity ρ_0 by means of a dressed Drude theory plasma frequency:

$$\Omega_p^2 = 4\pi\langle v_F\rangle^2 N(0)e^2/3 \tag{1}$$

and

$$\tau_{\text{tr}} = 4\pi/(\rho_0\Omega_p^2) \tag{2}$$

where $N(0)$ denotes the experimental or band structure quasiparticle density of states at the Fermi surface and $\langle v_F\rangle$ the Fermi velocity averaged over the Fermi surface.

It is obvious from this short description that any Fermi surface anisotropy enters into the theory of H_{c2} in a twofold way: firstly, via the electron–phonon coupling potential and, secondly, via the Fermi velocity. The success of the separable model for an anisotropic electron–phonon coupling spectral function

$$\alpha^2F(\omega)_{k,k'} = (1+a_k)\alpha^2F(\omega)(1+a_{k'}) \tag{3}$$

in the case of indium [12], suggested the application of the same model in an anisotropic theory of H_{c2}. (The indices k and k' represent the incoming and outgoing quasiparticle momentum vectors for the electron–phonon scattering process and a_k describes the deviation of the real Fermi surface in direction k from an isotropic one of the same volume.)

A similar ansatz has to be made consistently in order to describe the anisotropy of v_F and was indeed suggested by Teichler [19] in the form:

$$v_{F,k} = (1+b_k)\langle v_F\rangle \tag{4}$$

where b_k is defined similarly to a_k.

Equations (3) and (4) introduce two additional parameters: firstly, the mean square anisotropy $\langle a^2\rangle$ of the electron–phonon interaction and, secondly, the mean square anisotropy $\langle b^2\rangle$ of the Fermi velocity resulting in a temperature dependent gap anisotropy defined by [13]:

$$R^2 = \sum_n [\langle\Delta_k(n)^2\rangle - \langle\Delta_k(n)\rangle^2]\Big/\sum_n \langle\Delta_k(n)\rangle^2 \tag{5}$$

where $\langle\cdots\rangle$ denotes the Fermi surface average and $\Delta_k(n)$ are the Matsubara gaps in k direction in an imaginary axis representation.

As a result of the parameter study presented in Ref. 13, a suggestion was made about how to determine unambiguously the anisotropy parameters. This procedure seems to be perfectly applicable to the experimental data available for the set of niobium samples presented in Table I.

4. Results

In a first step the dependence of the critical temperature on the nitrogen content was analyzed to determine $\langle a^2\rangle$. This technique employs anisotropic linear Eliashberg equations [20] to determine $\langle a^2\rangle$ by calculating the T_c

degradation with increasing impurity concentration and by fitting to the experimental data. The basis of this procedure is the linear dependence of the impurity parameter $t^+ = 1/(2\pi\tau_{tr})$ on the residual resistivity ρ_0 according to equation (2). If we assume a niobium sample with a T_c of 9.305 K to be the 'clean' sample ($t^+ = 0$) and if we use the $\alpha^2F(\omega)$ data measured by Arnold et al. [21] we find

$$\langle a^2 \rangle = 0.0335 \pm 0.0035 \tag{6}$$

The mass enhancement factor λ is equal to 1.0 and the Coulomb pseudopotential μ^* is fitted to give the value of 0.204 for the above clean limit T_c. (The cut-off frequency we have chosen to be 174 meV $= 6\omega_D$.) This results in a variation of λ in the range

$$0.67 \leq \lambda \leq 1.4 \tag{7}$$

which agrees well with band structure calculations presented by Crabtree et al [22], where it is reported to vary in the range of $0.7 \leq \lambda \leq 1.29$.

In a second step, the theory of H_{c2} for anisotropic polycrystals in a two band model approximation is applied to analyze the experimental H_{c2} data of the polycrystalline samples. The paper by Crabtree et al [22] gives excellent advice on how to choose the parameters of such a model. Table IX of this reference suggests that a two band model is not unrealistic, because the λ values calculated for the octahedron and jungle gym parts of the Fermi surface are of about the same size, while the λ value for the ellipsoid is always significantly different. The octahedron and the jungle gym parts also make up about half of the Fermi surface, so it can be assumed that the two band model consists of two surface sheets of about the same weight. Furthermore, Fig. 14 of the same reference proves that the anisotropy functions a_k and b_k will have to have opposite signs on the same surface sheet, making λ large where v_F becomes small and vice versa.

Hence the further analysis is made along the following lines. From step one, each sample has been characterized by an unique value for the impurity parameter t^+, and the whole system by a specific value of $\langle a^2 \rangle$. Therefore we have two free parameters left, namely $\langle b^2 \rangle$ and $\langle v_F \rangle$. Both can easily be determined by fitting the theoretical results to the $H_{c2}(T)$ data of *one* arbitrary sample. A consistency check will then have to reproduce the $H_{c2}(T)$ data for all the other samples having no free parameter left. On the other hand, best possible fits can be made for the temperature dependence of H_{c2} for *each* sample. The corresponding variations in $\langle b^2 \rangle$ and $\langle v_F \rangle$ will allow then to assign 'error bars' for these two quantities.

If we choose, e.g., $\langle a^2 \rangle = 0.037$, the upper limit of the step one analysis, we find for $\langle b^2 \rangle$ and $\langle v_F \rangle$

$$\langle b^2 \rangle = 0.118 \pm 0.007 \tag{8}$$

$$\langle v_F \rangle = 0.57 \pm 0.01 \cdot 10^6 \text{ m/s}. \tag{9}$$

The errors are found by performing the best fit to each individual sample as mentioned above.

In Fig. 2 we compare the results of the theoretical predictions to the experimental data of the two samples Nb7 and Nb2 representing the two extreme polycrystals with respect to nitrogen content. We observe an almost perfect match between theory and experiment over the whole temperature range.

An even more sensitive check of the consistency between theory and experiment is provided by the anisotropy deviation function

$$D(t) = [H^a_{c2}(t)/H^i_{c2}(t) - 1] \cdot 100; t = T/T_c \tag{10}$$

where $H^i_{c2}(t)$ is the upper critical field of a *theoretical* isotropic system having the same T_c, t^+ and $\langle v_F \rangle$ as the real anisotropic system. Figure 3 presents $D(t)$ for all

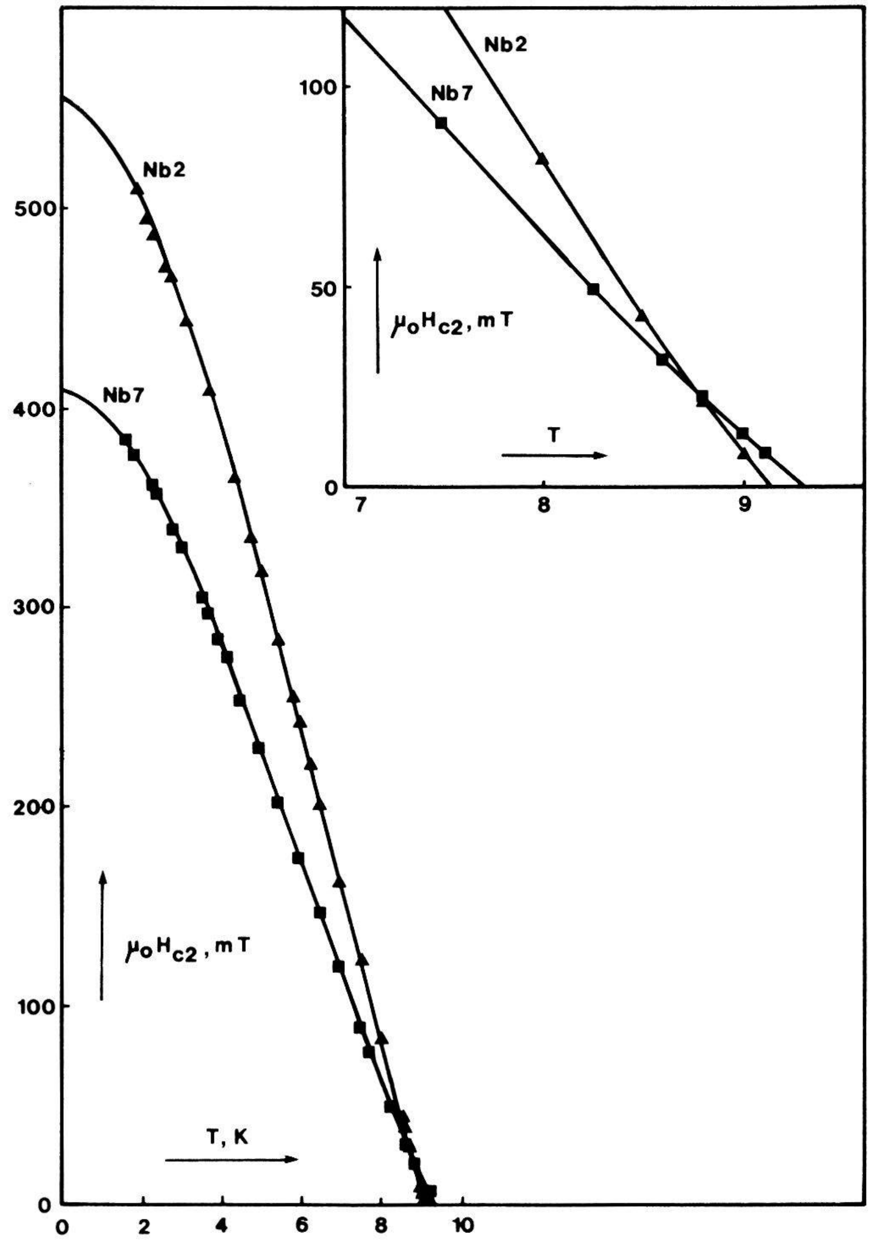

Figure 2
Temperature dependence of the upper critical fields in samples Nb7 and Nb2. The full curves represent theoretical results and the symbols refer to experimental data. (The insert shows the high temperature regime on an extended scale.)

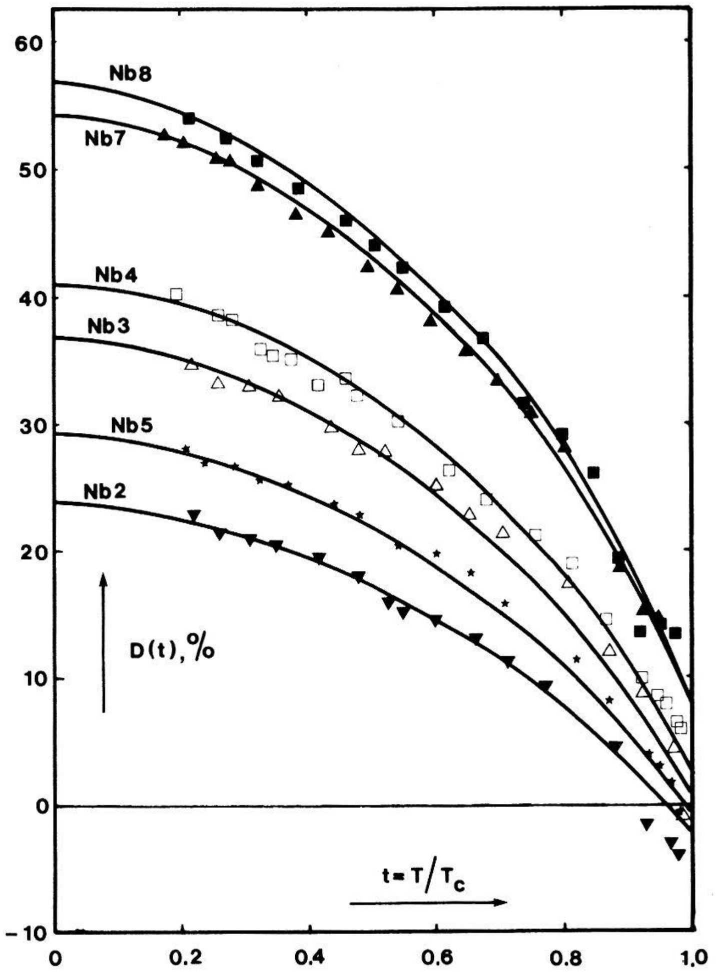

Figure 3
Anisotropy deviation function for the polycrystalline samples of Table I. The full curves correspond to the theoretical prediction in a best fit to the experimental data which are represented by symbols.

polycrystalline samples of Table I, in order to demonstrate the kind of agreement one can achieve between theory and experiment.

The value of $\langle v_F \rangle$ quoted in equation (9) is in excellent agreement with the band structure value of $0.62 \cdot 10^6$ m/s reported by Mattheis[23] and both values are in significant contrast to the value of $0.47 \cdot 10^6$ m/s found for sample Nb2 using the best possible fit for an *isotropic* theory [17]. The variation of v_F is in the range of

$$0.3735 \leq \langle v_F \rangle \leq 0.7645 \cdot 10^6 \text{ m/s} \tag{11}$$

which has to be compared with $0.3 \leq \langle v_F \rangle \leq 1.0 \cdot 10^6$ m/s as reported in Fig. 14 of Ref. 22.

The residual resistivity ρ_0 can now be calculated using equations (1, 2). A Sommerfeld constant γ of 7.8 mJ/(mole, K^2) [24, 25] together with a mass density of 8.606 g/cm^3 at 4.2 K results in a N(0) of $4.6 \cdot 10^{19}$ states/(cm^3, meV, spin) or 1.655 states/(eV, atom) (Crabtree et al. report a value of 1.45 states/(eV, atom) from band structure calculations) and gives a plasma frequency Ω_p of 8.83 eV. In Table I the theoretical values are compared to the experimental ones and again we note an extraordinarily good agreement, considering the crude model we were using to calculate ρ_0.

All these data result in a gap anisotropy of 15% at T_c for the cleanest sample Nb8 in excellent agreement with estimates made by Crabtree et al [22], who deduced an upper limit of 20% for the gap anisotropy from their data.

5. Conclusion

We have presented experimental as well as theoretical investigations of the temperature and impurity dependence of upper critical fields in niobium.

We find very strong evidence that the observed superconducting behaviour of niobium polycrystals with varying nitrogen content can be consistently explained by introducing a substantial anisotropy of the electron–phonon interaction and an even more substantial anisotropy of the Fermi velocity. This result contrasts somewhat the analysis presented by Butler [26], who assumed the Fermi velocity anisotropy to be dominant and thus neglected all other anisotropy contributions.

In conclusion we wish to point out that all the parameters needed to describe the experimental $H_{c2}(T)$ curves, i.e. the electron–phonon coupling anisotropy, the anisotropy of the Fermi velocity and its magnitude, agree very well with previous experimental and theoretical work on the Fermi surface of niobium.

Acknowledgements

This research was supported in part by Fonds zur Förderung der Wissenschaftlichen Forschung, Wien, under contract number 3973, 5032 and 6067P and by the Forschungsfonds of the Styrian Government.

REFERENCES

[1] H. W. Weber, Ed.: *Anisotropy Effects in Superconductors*, Plenum, New York (1977).
[2] M. L. A. MacVicar, J. L. Bostock and R. K. Milkove in Ref. 1, p. 257.
[3] E. Seidl, H. W. Weber and H. Teichler, J. Low Temp. Phys. *30*, 273 (1978).
[4] E. Moser, E. Seidl and H. W. Weber, J. Low Temp. Phys. *49*, 585 (1982).
[5] E. Moser, E. Seidl, H. W. Weber and E. Schachinger in: *Superconductivity in d- and f-Band Metals*, ed.: W. Buckel and W. Weber, Kernforschungszentrum Karlsruhe, 1982, p. 519.
[6] F. M. Sauerzopf, E. Moser, H. W. Weber and F. A. Schmidt, J. Low Temp. Phys. *66*, 191 (1987).
[7] P. W. Anderson, J. Phys. Chem. Sol. *11*, 26 (1959).
[8] D. Markowitz and L. P. Kadanoff, Phys. Rev. *131*, 563 (1963).
[9] G. Bergmann and D. Rainer, Z. Phys. *236*, 59 (1973).
[10] J. M. Daams and J. P. Carbotte, J. Low Temp. Phys. *43*, 263 (1981).
[11] W. H. Butler and P. B. Allen, in: *Superconductivity in d- and f-Band Metals, ed.*: D. H. Douglas, Plenum, New York (1976), p. 73.
[12] L. Niel, N. Giesinger, H. W. Weber and E. Schachinger, Phys. Rev *B32*, 2976 (1985).
[13] M. Prohammer and E. Schachinger, Phys. Rev. *B36*, 8353 (1987).
[14] M. Prohammer, Solid State Commun. (in print).
[15] P. Hahn and H. W. Weber, Cryogenics *23*, 87 (1983).
[16] N. R. Werthamer, E. Helfand and P. C. Hohenberg, Phys. Rev. *158*, 415 (1967).

[17] M. SCHOSSMANN and E. SCHACHINGER, Phys. Rev. *B33,* 6123 (1986).
[18] M. PETER, J. ASHKENAZI and M. DACOROGNA, Helv. Phys. Acta *50* , 267 (1977).
[19] H. TEICHLER, in Ref. 1, p. 75.
[20] J. M. DAAMS, E. SCHACHINGER and J. P. CARBOTTE, J. Low Temp. Phys. *42*, 69 (1981).
[21] G. B. ARNOLD, J. ZASADZINSKI, J. W. OSMUN and E. L. WOLF, J. Low Temp. Phys. *40*, 225 (1980).
[22] G. W. CRABTREE, D. H. DYE, D. P. KARIM, S. A. CAMPBELL and J. B. KETTERSON, Phys. Rev. *B35,* 1728 (1987).
[23] L. F. MATTHEIS, Phys. Rev. *B1,* 373 (1970).
[24] D. ECKERT, Diploma Thesis, University of Geneva (1983), unpublished.
[25] B. J. C. VAN DER HOEVEN, JR. and P. H. KEESOM, Phys. Rev. *134*, A1320 (1964).
[26] W. H. BUTLER, Phys. Rev. Lett. *44*, 1516 (1980).